Journal of Engineering Mathematics, Vol. 6, No. 3, July 1972
Wolters-Noordhoff Publishing–Groningen
Printed in the Netherlands

Diffraction of A Plane Pulse by A Three-Dimensional Corner*

L. TING AND F. KUNG

Department of Mathematics and Aerospace Laboratory, New York University, Bronx, New York 10453, *U.S.A.*

(Received August 31, 1971)

SUMMARY

The conical solutions for the incidence of a plane pulse on a three-dimensional corner are presented. The corner is represented by a trihedron with one edge perpendicular to the other two. Both the boundary condition of the first kind, $p=0$, and that of the second kind, $\partial p/\partial n=0$, are considered. Outside the characteristic sphere of the vertex of the corner, the solution is represented by the well known conical solutions in two variables. Inside the characteristic sphere, the problem involves three conical variables. By the separation of variables, the problem is reduced to that of an eigenvalue problem with an irregular boundary which is in turn reduced to a system of homogeneous algebraic equations. The eigenvalues are then determined numerically. By the superposition of the conical solutions for plane pulses, the solution for the incidence of a plane wave is obtained. Numerical examples simulating the incidence of a sonic boom on the corner of a structure are presented.

1. Introduction

The problem of diffraction and reflection of acoustic waves or electromagnetic waves by wedges, corners and other two-dimensional or axially symmetric obstacles has received extensive investigations. A survey of these investigations can be found in [1].

A canonical two-dimensional problem is the diffraction of a plane pulse by a wedge or corner. Explicit solutions in terms of elementary functions were obtained by Keller and Blank [2] for the boundary condition of the first kind, $p=0$, and for that of the second kind, $\partial p/\partial n=0$. The corresponding solutions are applicable respectively to a single component of electric field or magnetic field with a perfect conducting wedge or corner. They are also applicable to acoustic pressure with free or rigid walls respectively. The explicit solutions are obtainable because (i) the absence of a length scale allows the reduction of three variables x, y, t to two conical variables x/t and y/t, (ii) the law of propagation of discontinuities [3] converts the initial boundary value problem to a boundary value problem in conical variables, and (iii) the Busemann conical transformation [4] converts the governing equation to Laplace equation and allows the use of conformal mapping.

In this paper, the solution for a canonical three-dimensional diffraction problem is presented. The problem is the diffraction of a plane pulse by a three-dimensional corner. Both the boundary condition of the first kind and that of the second kind will be considered. The corner is represented by a trihedron with one edge perpendicular to the other two. The corner of a cube is a special example. Due to the absence of a length scale for a trihedron, the solutions is conical in three variables $\zeta=r/(Ct)$, θ and φ where r, θ, φ are the spherical coordinates with origin located at the vertex of the trihedron. For a trihedron the three-dimensional effect is confined inside the characteristic sphere $r=Ct$ or the unit sphere $\zeta=1$. Outside the unit sphere, the solution is two-dimensional and can be represented by the known conical solutions in two variables [2]. From the law of propagation of discontinuities [3], the solution outside the unit sphere provides the boundary data on the unit sphere and the original initial boundary value problem of the three-dimensional wave equation is converted to a boundary value problem in conical variables ζ, φ and θ in section 2. The geometrical restriction that one edge of the trihedron is perpendicular to the other two enables the separation of the variable ζ from θ and φ and the associated eigenvalue problem in θ–φ plane is defined.

* This work was supported by NASA Grant No. NGL-33-016-119.

In section 3, a procedure is presented such that the eigenvalue problem for either the boundary condition of the first kind or of the second kind is reduced to a system of linear algebraic equations. Numerical results for the eigenvalues and eigenfunctions are obtained and they are applied to construct the conical solution for the diffraction of a plane pulse in section 4. By the decomposition of a plane wave to plane pulses, the diffraction of a plane wave by a three-dimensional corner is presented in section 5.

2. Formulation of the Three-Dimensional Conical Problem

For the acoustic disturbance pressure p, or a component of the electric or magnetic field, the governing differential equation is the simple wave equation,

$$p_{xx}+p_{yy}+p_{zz}-C^{-2}p_{tt}=0 \tag{1}$$

where C is the speed of propagation in the region outside a trihedron simulating a three-dimensional corner. As shown in Fig. 1, two edges, OA and OB, of the trihedron are in the x–y plane and are bisected by the negative x-axis with half angle α and the third edge OD, which is the negative z-axis with the vertex 0 as the origin. Let $t=0$ be the instant when the pulse front hits the vertex. In order to carry out the formulation for the boundary condition of the first kind and of the second kind simultaneously, an index h will be introduced with $h=0, 1$ for the first and the second kind respectively. The boundary condition on the three faces of the trihedron is

$$\partial^h p/\partial n^h = 0 \tag{2}$$

The three-dimensional disturbance due to the vertex is confined inside the sphere $r=Ct$ where $r=(x^2+y^2+z^2)^{\frac{1}{2}}$. Outside the sphere, the solution is given either by the regular reflection of the plane pulse from the surfaces of the trihedron or by the diffraction of the pulse by the edges. When the pulse front is parallel to the edge, the diffracted wave is given by a two-dimensional unsteady conical solution. When the pulse front is not parallel to the edge, the diffracted wave is given by a steady three-dimensional conical solution. For both cases, solutions are given in two conical variables in [2] by means of Busemann's conical flow method.

Due to the absence of a time scale and a length scale, the disturbance p, non-dimensionalized by the strength of the incident pulse, should be a function of three conical variables, $x/(Ct)$, $y/(Ct)$ and $z/(Ct)$ or in terms of the spherical coordicates by $\zeta=r/(Ct)$, θ and φ. The simple wave equation for $p(\zeta, \theta, \varphi)$ becomes,

$$\zeta^2(1-\zeta^2)\frac{\partial^2 p}{\partial \zeta^2}+2\zeta(1-\zeta^2)\frac{\partial p}{\partial \zeta}+\frac{1}{\sin\theta}\frac{\partial}{\partial\theta}\left(\sin\theta\frac{\partial p}{\partial\theta}\right)+\frac{1}{\sin^2\theta}\frac{\partial^2 p}{\partial\varphi^2}=0 \tag{3}$$

inside the unit sphere, $\zeta=1$, and exterior to the trihedron. The boundary conditions are:

$$\partial^h p/\partial\theta^h=0 \quad \text{on surface OAB, } \theta=\pi/2,\ -(\pi-\alpha)<\varphi<\pi-\alpha \tag{4}$$

$$\partial^h p/\partial\varphi^h=0 \quad \text{on surface OAD, } \varphi=\pi-\alpha,\ \pi/2<\theta<\pi \tag{5a}$$

$$\partial^h p/\partial\varphi^h=0 \quad \text{on surface OBD, } \varphi=-\pi+\alpha,\ \pi/2<\theta<\pi \tag{5b}$$

and $p=F(\theta, \varphi)$ on unit sphere $\zeta=1$ outside of the trihedron.

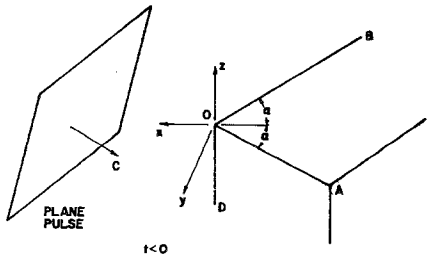

Figure 1. Incidence of a plane pulse on a corner.

The jump across the sphere is inversely proportional to the square root of the area of the ray tube, $(dS)^{\frac{1}{2}}$. Since all the rays reaching the sphere come from the origin where $dS_0 = 0$, the jump across the sphere is zero. The pressure is continuous across the sphere $\zeta = 1$; and $F(\theta, \varphi)$ is defined by the solutions outside the sonic sphere in two conical variables given by [2].

To construct the solution by the method of separation of variables, the usual trial substitution $p(\zeta, \theta, \varphi) = A(\zeta) G(\mu, \varphi)$ is introduced where $\mu = \cos\theta$ and equation (3) becomes

$$\zeta^2(1-\zeta^2)Z''(\zeta) + 2(1-\zeta^2)\zeta Z'(\zeta) - \lambda(\lambda+1)Z(\zeta) = 0 \tag{6}$$

for $1 > \zeta \geqq 0$, and

$$\frac{\partial}{\partial\mu}\left[(1-\mu^2)\frac{\partial G}{\partial\mu}\right] + \lambda(\lambda+1)G + \frac{1}{1-\mu^2}\frac{\partial^2 G}{\partial\varphi^2} = 0 \tag{7}$$

for the domain in μ–φ plane with $|\varphi| < \pi - \alpha$ when $0 \geqq \mu \geqq -1$, and with $|\varphi| \leqq \pi$ when $1 \geqq \mu > 0$. Since p and also G are single valued, G should be periodic in φ when $1 \geqq \mu > 0$, i.e.

$$G(\mu, \varphi + 2\pi) = G(\mu, \varphi)\,. \tag{8}$$

The range of φ is therefore restricted from $-\pi$ to π and the two ends are connected by the periodicity condition.

The replacement of the variable θ by μ and the use of the constant of separation $\lambda(\lambda+1)$ are motivated by the intention of representing $G(\mu, \theta)$ by the spherical harmonics.

The boundary conditions on the surfaces of the trihedron, eq. (4), become

$$\partial^h G/\partial\mu^h = 0 \text{ along } \mu = 0 \text{ with } \pi - \alpha < |\varphi| \leqq \pi \tag{9a}$$

$$\partial^h G/\partial\varphi^h = 0 \text{ along } \varphi = \pm(\pi - \alpha) \text{ with } -1 < \mu < 0 \tag{9b}$$

The condition that p is bounded in particular at the two poles, $\theta = 0$ and $\theta = \pi$, yields the condition,

$$|G| < \infty \text{ at } \mu = \pm 1 \tag{9c}$$

The periodicity condition, eq. (8), supplies the condition along the remaining boundaries,

$$G(\mu, -\pi) = G(\mu, \pi) \text{ and} \tag{9d}$$

$$G_\varphi(\mu, -\pi) = G_\varphi(\mu, \pi) \text{ for } 1 \geqq \mu > 0\,.$$

The differential equation (7) and the boundary conditions (9a–d), define an eigenvalue problem. The determination of the eigenvalues, λ's, and the associated eigenfunctions, $G_\lambda(\mu, \varphi)$ are described in the next section.

3. The Eigenvalue Problem

For the eigenvalue problem formulated in the preceding section, two edges of the trihedron, OA and OB, are assumed to be normal to the third edge. This restriction is imposed due to two considerations: (1) the surfaces of the corner can be defined by surfaces of constant θ or constant φ's and (2) the solutions outside the unit sphere for the diffraction problem can be constructed as solutions of two-dimensional problems [2]. For the solution of the eigenvalue problem itself the second consideration is irrelevant. The eigenvalue problem in this section will, therefore, be formulated for a wider class of corners as shown in Fig. 2. The surface OAB is a conical surface with $\theta = \beta$ and the two surfaces OAD and OBD are planes with $\varphi = \pi - \alpha$ and $\varphi = -\pi + \alpha$ respectively. The boundary conditions for the solution of eq. (7) are

$$\partial^h G/\partial\mu^h = 0 \text{ along } \mu = \mu_0 = \cos\beta \text{ with } \pi - \alpha < |\varphi| \leqq \pi \tag{10a}$$

$$\partial^h G/\partial\varphi^h = 0 \text{ along } \varphi = \pm(\pi - \alpha) \text{ with } -1 \leqq \mu < \mu_0 \tag{10b}$$

$$|G| < \infty \text{ at } \mu = \pm 1 \tag{10c}$$

$$G(\mu, \pi) = G(\mu, -\pi), \quad G_\varphi(\mu, \pi) = G_\varphi(\mu, -\pi) \quad \text{for} \quad \mu_0 < \mu \leqq 1. \tag{10d}$$

For the special case of $\beta=\pi/2$, or $\mu_0=0$, the boundary conditions of eqs. (10a–d) and the domain in the $\mu-\varphi$ plane (Fig. 2) reduce to those of eqs. (9a–d).

The eigenvalue problem is now defined by the differential eq. (7) and the boundary conditions (10a–d). In order to reduce the problem to that for a set of algebraic equations, two representations of the eigenfunction $G_\lambda(\mu, \varphi)$ associated with the eigenvalue λ will be sought; one for the region, R^+, with $\mu > \mu_0$ and the other for R^- with $\mu < \mu_0$ (Fig. 2). These two solutions and their normal derivatives will be matched across the dividing line $\mu=\mu_0$ for $|\varphi| < \pi-\alpha$.

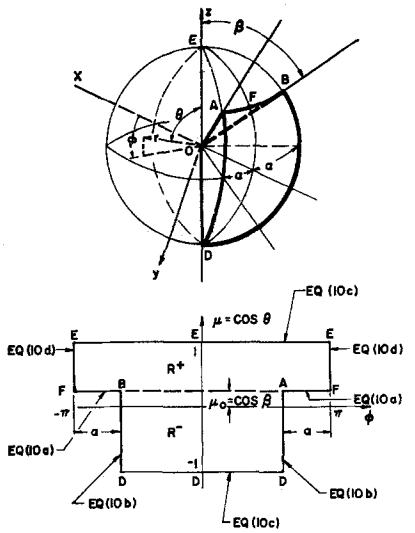

Figure 2. Eigenvalue problem for the corner.

For the upper region R^+, the eigenfunction $G_\lambda^+(\mu, \varphi)$ which is periodic in φ on account of eq. (10d) or eq. (8) can be represented by the Fourier series in φ with period of 2π,

$$G_\lambda^+(\mu, \varphi) = \sum_{m=0,1,\ldots} A_m p_\lambda^{-m}(\mu) \cos m\varphi + \sum_{m=1,2,\ldots} B_m p_\lambda^{-m}(\mu) \sin m\varphi \,. \tag{11}$$

For each m, eq. (7) yields the Legendre equation for $p_\lambda^{-m}(\mu)$

$$\frac{d}{d\mu}\left[(1-\mu^2)\frac{d}{d\mu} p_\lambda^{-m}(\mu)\right] + \left[\lambda(\lambda+1) - \frac{m^2}{1-\mu^2}\right] p_\lambda^{-m}(\mu) = 0 \,. \tag{12}$$

Since eq. (11) is defined for $1 \geqq \mu \geqq \mu_0 > -1$, p_λ^{-m} should be finite at $\mu=1$. p_λ^{-m} is identified as the generalized Legendre function [5] and defined by

$$p_\lambda^{-m}(\mu) = \left(\frac{1-\mu}{1+\mu}\right)^{m/2} F\{-\lambda, \lambda+1, 1+m; (1-\mu)/2\} \tag{13}$$

where F denotes the Gaussian hypergeometric function. The factor $1/\Gamma(1+m)$ is omitted on the right side of eq. (13) since it is automatically absorbed into coefficients A_m and B_m with a net saving of programming and computing time.

For the lower region R^-, i.e., $-1 \leqq \mu < \mu_0$ the eigenfunction G_λ^-, which fulfills the boundary conditions of eqs. (10b and c), can be expressed as a sine or a cosine series in $(\varphi+\pi-\alpha)$ with half period of $2(\pi-\alpha)$ for $h=0$ or 1 respectively, i.e.

$$G_\lambda^-(\mu, \varphi) = \Sigma\, E_n P_\lambda^{-(n\pi/\Phi)}(-\mu) \sin\left[\frac{n\pi}{\Phi}\left(\varphi + \frac{\Phi}{2}\right) + \frac{\pi h}{2}\right]$$

where $\Phi=2(\pi-\alpha)$ and the summation is over all integers $n \geqq 1-h$. Similarly for each n, eq. (7) becomes the Legendre equation and $P_\lambda^{-n\pi/\Phi}(-\mu)$ is the generalized Legendre function. The argument is $-\mu$ so that the function is finite for $-1 \leqq \mu \leqq \mu_0 < 1$. In the series for G_λ^-, the

terms are alternately even and odd functions of φ. The series can be written as the sum of an even and an odd series,

$$G_\lambda^-(\mu,\varphi)=\sum_{j=0,1\ldots} C_j P_\lambda^{-\bar{\nu}_j}(-\mu)\cos\nu_j\varphi+\sum_{j=1,2\ldots} D_j P_\lambda^{-\bar{\nu}_j}(-\mu)\sin\bar{\nu}_j\varphi \tag{14}$$

where

$$\nu_j=(2j+1-h)\pi/\Phi\,,\quad \bar{\nu}_j=(2j-h)\pi/\Phi,\quad C_j=E_{2j}(-1)^j \text{ and } D_j=E_{2j-1}(-1)^j\,.$$

Both expressions (11) and (14) fulfill the differential equation (7) and the boundary conditions (10b-d) appropriate for regions R^+ and R^- respectively.

Across the dividing line of R^+ and R^-, where $\mu=\mu_0$ and $|\varphi|<\pi-\alpha$, the matching conditions are the continuity of the eigenfunctions G_λ and its normal derivative $\partial G_\lambda/\partial\mu$. The continuity of the second derivatives are then assured since both G_λ^+ and G_λ^- fulfill the same differential equation (7). The matching conditions are:

$$G_\lambda^+(\mu_0^+,\varphi)=G_\lambda^-(\mu_0^-,\varphi)\quad\text{for}\quad|\varphi|\leqq\pi-\alpha \tag{15}$$

and

$$\partial G_\lambda^+(\mu_0^+,\varphi)/\partial\mu=\partial G_\lambda^-(\mu_0^-,\varphi)/\partial\mu\quad\text{for}\quad|\varphi|<\pi-\alpha\,. \tag{16}$$

The remaining boundary condition, eq. (10a) becomes

$$\partial^h G_\lambda^+(\mu_0^+,\varphi)/\partial\mu^h=0\quad\text{for}\quad\pi-\alpha<|\varphi|\leqq\pi\,. \tag{17}$$

It should be pointed out here that although the eigenfunctions are continuous, its derivatives may not exist along the edges. The singularity along the edge $\theta=\pi$ is built in by the representation for $G^-(\mu,\varphi)$. The singularity along the edges, $\theta=\beta$ and $\varphi=\pm(\pi-\alpha)$ can be ascertained by investigating the behavior of the solutions of the differential equations for $G(\mu,\varphi)$, eq. (7). In the neighborhood of an edge, i.e., $|\tilde{\mu}|\ll 1$ and $|\tilde{\varphi}|\ll 1$ with $\tilde{\mu}=\mu_0-\mu$, $\tilde{\varphi}=\pi-\alpha-\varphi$, eq. (7) can be approximated by the Laplace equation

$$(1-\mu_0^2)^2\,\partial^2 G/\partial\tilde{\mu}^2+\partial^2 G/\partial\tilde{\varphi}^2=0$$

in the first three quadrants of the $\tilde{\mu}$–$\tilde{\varphi}$ plane subjected to the boundary condition that $\partial^h G/\partial n^h$ vanishes along the positive $\tilde{\mu}$-axis and along the negative $\tilde{\varphi}$-axis. The solution G near the origin $\tilde{\mu}=\tilde{\varphi}=0$ should behave as the real or the imaginary part of $[\tilde{\mu}(1-\mu_0^2)^{-1}+i\tilde{\varphi}]^{\frac{1}{3}}$ for $h=1$ or 0 respectively [6]. The same result can be obtained by observing the three-dimensional corner directly: the surfaces of $\varphi=\pi-\alpha$ and $\theta=\beta$ intersect at right angle and in the neighbourhood of the edge away from the vertex, the solution behaves as that of a two-dimensional convex right corner.

Along the interface of G^+ and G^-, i.e., $\tilde{\mu}=\mu_0=0$ and $\tilde{\varphi}>0$, the normal derivative of G behaves as the real or the imaginary part of $(\tilde{\varphi}i)^{-\frac{1}{3}}$ for $h=1$ or 0 respectively. For either case, the behavior of G_μ is $G_\mu(\mu=\mu_0,\varphi\to\pi-\alpha-0)\sim(\pi-\alpha-\varphi)^{-\frac{1}{3}}$. G_μ is singular near the edge but is square integrable for the appropriate interval of φ, namely $-\pi<\varphi<\pi$ for G^+ when $\mu>\mu_0$ and $-(\pi-\alpha)<\varphi<\pi-\alpha$ for G^- when $\mu<\mu_0$.

3.1. *Reduction to Algebraic Equations*

Equations (15, 16 and 17) will now be reduced to a system of linear homogeneous algebraic equations for the unknowns A_m, B_m, C_j and D_j by the following procedure.

For the boundary condition of the first kind ($h=0$), eqs. (15) and (17) together define $G^+(\mu_0,\varphi)$ for $|\varphi|\leqq\pi$. For the boundary condition of the second kind ($h=1$), eqs. (16) and (17) together define $G_\mu^+(\mu_0,\varphi)$ for the same interval. Since G^+ is represented by the Fourier series of eq. (11), the combined equation for each case, i.e., eqs. (15 and 17) for $h=0$ or eqs. (16 and 17) for $h=1$, will be multiplied by an even component $\cos n\varphi$ and integrated over the interval $(-\pi,\pi)$. The result is an algebraic equation for the even coefficients A_m and C_j for each integer n,

$$A_n[\partial^h P_\lambda^{-n}(\mu_0)/\partial\mu^h][1+\delta_{0n}]-(-1)^h\sum_{j=0,1\ldots} C_j[\partial^h P_\lambda^{-\nu_j}(-\mu_0)/\partial\mu^h]I_{jn}=0$$
$$\text{for } n=0,1,2\ldots \tag{18}$$

where

$$I_{jn} = \frac{1}{\pi}\int_{-\Phi/2}^{\Phi/2} \cos \nu_j\varphi \cos n\varphi \, d\varphi$$
$$= \Phi[1+h\delta_{0n}]/(2\pi), \qquad \nu_j = n$$
$$= \frac{2(-1)^i[nh+\nu_j(1-h)]}{\pi(\nu_j^2-n^2)} \cos\frac{(n\varphi+h\pi)}{2}, \qquad \nu_j \neq n \tag{19}$$

The remaining equation, i.e. eq. (16) for $h=0$ or eq. (15) for $h=1$, defines $\partial^h G^-(\mu_0, \varphi)/\partial\mu^h$ for the interval $-\Phi/2 < \varphi < \Phi/2$. That equation will be multiplied by an even component $\cos \nu_k\varphi$ in the Fourier series for G^- with $\nu_k = (2k+1-h)\pi/\Phi$ and be integrated over the interval $(-\Phi/2, \Phi/2)$. The result is

$$\sum_{m=0,1,\ldots} A_m[\partial^{1-h}P_\lambda^{-m}(\mu_0)/\partial\mu^{1-h}]I_{km} + (-1)^h C_k[\partial^{1-h}P_\lambda^{-\nu_k}(-\mu_0)/\partial\mu^{1-h}]$$
$$\Phi(1+h\delta_{0k})/2\pi = 0$$
$$\text{for } k=0, 1, 2\ldots \tag{20}$$

When the even components $\cos n\varphi$ and $\cos \nu_k\varphi$ are replaced by the odd components $\sin n\varphi$ and $\sin \bar{\nu}_k\varphi$ respectively in the derivation of eqs. (18) and (20) from eqs. (15, 16 and 17), those two equations become the following two equations for the odd coefficients B_m and D_j. They are:

$$B_n[\partial^h P_\lambda^{-n}(\mu_0)/\partial\mu^h] - (-1)^h \sum_{j=1,2\ldots} D_j[\partial^h P_\lambda^{-\bar{\nu}_j}(-\mu_0)/\partial\mu^h]L_{jn} = 0$$
$$\text{for } n=1, 2, \ldots \tag{21}$$

and

$$\sum_{m=1,2\ldots} B_m[\partial^{1-h}P_\lambda^{-m}(\mu_0)/\partial\mu^{1-h}]L_{km} + (-1)^h D_k[\partial^{1-h}P_\lambda^{-\bar{\nu}_j}(-\mu_0)/\partial\mu^{1-h}]\Phi/(2\pi) = 0$$
$$\text{for } k=1, 2, \ldots \tag{22}$$

where

$$L_{jn} = \frac{1}{\pi}\int_{-\Phi/2}^{\Phi/2} \sin \bar{\nu}_j\varphi \sin n\varphi \, d\varphi$$
$$= \begin{cases} \Phi/(2\pi) & \bar{\nu}_j = n \\ \dfrac{2[\bar{\nu}_j(1-h)+nh]}{\pi(\bar{\nu}_j^2-n^2)}(-1)^{n+1}\sin\dfrac{n\Phi+h\pi}{2}, & \bar{\nu}_j \neq n \end{cases} \tag{23}$$

The eigenvalue problem is now uncoupled, with eqs. (18) and (20) for the even solutions and eqs. (21) and (22) for the odd solutions. The numerical solution to those homogeneous algebraic equations will be described in the next sub-section.

3.2. *Numerical Solutions*

To obtain the numerical solutions, the infinite cosine series in eq. (11), the even part of G_λ^+, will be truncated with maximum $m=M_c$. Similarly the cosine series in eq. (17), the even part of G_λ^-, will be truncated with maximum $j=J_c$. Likewise, M_c and J_c will be the maximums of n and k, respectively, so that eqs. (18) and (20) yield M_c+J_c+2 linear homogeneous equations for the M_c+J_c+2 constants $A_0, A_1, \ldots, A_{M_c}$ and $C_0, C_1, \ldots, C_{J_c}$. These solutions are nontrivial if λ is a root of the characteristic equation,

$$\Delta_c(\lambda) = \det(Q) = 0 \tag{24}$$

where Q is an $(M_c+J_c+2)\times(M_c+J_c+2)$ square matrix. Its elements are the coefficients of the unknowns $A_0, A_1, \ldots, A_{M_c}$, and $C_0, C_1, \ldots, C_{J_c}$ in M_c+1 equations from eq. (18) with $n=0, 1, \ldots, M_c$ and J_c+1 equations from eq. (20) with $k=0, 1, \ldots, J_c$.

The search for the eigenvalue λ can be restricted to the half plane, real part $\lambda \geqq -\frac{1}{2}$, because the eigenfunction is invariant with respect to the product $\lambda(\lambda+1)$ which is symmetric about $\lambda=-\frac{1}{2}$. Since the differential equation, eq. (7), and the boundary conditions, eqs. (10a-d), are self-adjoint, the product $\lambda(\lambda+1)$ must be real, i.e. $\lambda(\lambda+1)-\bar{\lambda}(\bar{\lambda}+1)=(\lambda-\bar{\lambda})(\lambda+\bar{\lambda}+1)=0$. Therefore the eigenvalues will lie on the real axis with $\lambda=\bar{\lambda}\geqq-\frac{1}{2}$ or lie on the line, Re $\lambda=(\lambda+\bar{\lambda})/2=-\frac{1}{2}$. For given λ, it is shown in the next sub-section that the differential equation for $Z(\zeta)$, eq. (16), does not admit a solution finite at the origin ($\zeta=0$) when Re $\lambda<0$. The search for the eigenvalue λ can therefore be restricted to the positive real axis, i.e., $\lambda=\bar{\lambda}\geqq 0$.

For given values of M_c and I_c, the eigenvalues are the roots of $\Delta_c(\lambda)=0$. The real positive roots of $\Delta_c(\lambda)=0$ can be located by numerical evaluation of $\Delta_c(\lambda)$ as a function of real positive λ. When the derivative of $\Delta_c(\lambda)$ at a root is non zero, the coefficients A_m, C_j are proportional to the cofactors of the determinant, i.e.,

$$\begin{aligned} A_m &= N^{-1} Q_{1,M+1} \quad \text{for} \quad M=0, 1, 2, \ldots, M_c \\ C_j &= N^{-1} Q_{1,M_c+1+j} \quad \text{for} \quad j=0, 1, 2, \ldots, J_c \end{aligned} \tag{25}$$

where Q_{1i} is the cofactor of the element q_{1i} of the determinant. The constant N is defined by the normalization condition,

$$\int_{\mu_0}^{1} d\mu \int_0^{\pi} d\varphi \,[G_\lambda^+(\mu,\theta)]^2 + \int_{-1}^{\mu_0} d\mu \int_0^{\Phi/2} d\varphi \,[G_\lambda^-(\mu,\theta)]^2 = 1 \tag{26}$$

The equation for N is

$$\begin{aligned} N^2 = {} & \frac{\pi}{2} \int_{\mu_0}^{1} d\mu \sum_{m=0}^{M_c} [P_\lambda^{-m}(\mu) Q_{1,m+1}]^2 (1+\delta_{0m}) \\ & + \frac{\Phi}{4} \int_{-\mu_0}^{1} d\mu \sum_{j=0}^{J_c} [P_\lambda^{-\nu_j}(\mu) Q_{1,M_c+1+j}]^2 (1+\delta_{0j}) . \end{aligned} \tag{27}$$

Similarly for the odd solutions, the series in eqs. (11) and (17) will be truncated with maximum $m=M_s$ and maximum $j=J_s$ respectively. There will be M_s equations for eq. (21) and M_j equations for eq. (22). The roots of the characteristic equation yield the eigenvalues for the odd solutions. The ratios of the cofactors and the normalization condition of eq. (26) define the coefficients $B_1 \ldots B_{M_s}$ and $D_1 \ldots D_{J_s}$ in the eigenfunctions.

It should be pointed out here that the convergence of the eigenvalues and eigenfunctions of the truncated problem has been assumed and the equivalence between the matching conditions of eqs. (15) and (16) and the matching of the Fourier coefficients is also assumed. Some confidence in these assumptions will be offered by the following numerical results.

For the special case of a two-dimensional corner, namely $\alpha=\pi/2$, $\beta=\pi/2$ in Fig. 2, the eigenvalue problem can be solved exactly by choosing the edge of the corner as the $\bar{z}$-axis (Fig. 3).

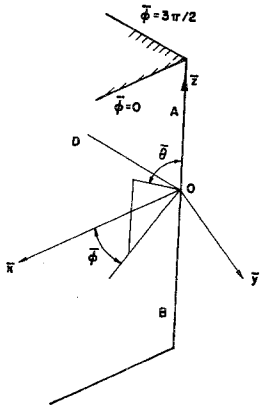

Figure 3. A two-dimensional corner.

In spherical coordinates $\bar{\theta}$ and $\bar{\varphi}$, the two sides are $\bar{\varphi}=0$ and $\bar{\varphi}=3\pi/2$. The eigenfunction can be written as

$$\bar{G}_\lambda(\bar{\theta}, \bar{\varphi}) = P_\lambda^{-2j/3}(\bar{\mu}) \sin[(2j/3)\bar{\varphi}+h\pi/2] \tag{28}$$

where $\bar{\mu}=\cos\bar{\theta}$ and $j=0, 1, 2, \ldots$. For $h=0$, the solution corresponding to $j=0$ is trivial. The eigenvalue λ is defined by the condition that $P_\lambda^{-2j/3}$ should be finite at $\bar{\theta}=\pi$ or $\bar{\mu}=-1$. Instead of eq. (13), an equivalent expression for $P_\lambda^{-\nu}(\bar{\mu})$ is [5],

$$P_\lambda^{-\nu}(\bar{\mu}) = 2^{-\nu}(1-\bar{\mu}^2)^{\nu/2} F(\nu-\lambda, \nu+\lambda+1, \nu+1; X) \tag{29}$$

where

$$\nu=2j/3 \quad \text{and} \quad X=(1-\bar{\mu})/2 .$$

The power series representation for the hypergeometric function is divergent at $X=1$ or $\bar{\mu}=-1$ unless the series has only finite number of terms, say $k+1$ terms. The condition for λ is

$$\nu-\lambda+k=0 \quad \text{or} \quad \lambda_{jk}=k+2j/3 . \tag{30}$$

For $j=0, 1, 2, 3, \ldots$, the eigenvalues are $\lambda_{0,k}=0, 1, 2, 3, \ldots$, $\lambda_{1,k}=\frac{2}{3}, \frac{5}{3}, \frac{8}{3}, \ldots$, $\lambda_{2,k}=\frac{4}{3}, \frac{7}{3}, \ldots$, $\lambda_{3,k}=2, 3, \ldots$, $\lambda_{4,k}=\frac{8}{3}, \ldots$. For the case $h=0$, $\lambda_{0,k}$ are not eigenvalues because those eigenfunctions are trivial.

The numerical program developed for the general eigenvalue problem is tested by setting $\beta=\pi/2$ and $\alpha=\pi/2$ and the eigenvalues between 0 and 3 for the boundary condition of the first and second kind ($h=0, 1$) respectively are obtained for various combinations of M_c, J_c, M_s and J_s. For the combination of $M_c=8, J_c=4, M_s=9$ and $J_s=5$ the eigenvalues given by the numerical program are in agreement with the exact values of eq. (30) within 0.2%. When the numbers of M's and J's are increased, the accuracy improves. This is a confirmation of the procedure developed in this paper and the numerical program for the eigenvalue problem.

Since the eigenvalues of the truncated problem are assumed to converge as M and J increase simultaneously, their limits should be independent of the differences between M and J where M and J stand for M_c, J_c, or M_s, J_s, i.e., the differences between the number of terms in the series for G^+ and that for G^-. This fact is also confirmed by all the available numerical results. Nevertheless, a rule for the optimum difference between M and J for a given $M+J$ and its justification are presented in [7]. The required total number $M+J$ for a given degree of accuracy (say 0.2% error in the eigenvalues) is decided by comparing the results with those with a larger $M+J$ as described in [7].

For the corner of a cube, i.e., $\alpha=\pi/4$ and $\beta=\pi/2$, some of the eigenvalues and eigenfunctions can be found exactly by picking out those spherical harmonic functions, $P_m^n(\mu)\exp(in\varphi)$ with $n \leqq m$, which fulfills the boundary conditions on the three faces of the corner. From the boundary condition on the top surface ($\mu=0$) it is clear that all the odd integers are eigenvalues for the boundary condition of the first kind ($h=0$) and all the even integers are eigenvalues for the second kind ($h=1$). These exact eigenvalues are

$$\lambda = m = 2k+1-h \quad \text{for} \quad k=0, 1, 2, 3, \ldots . \tag{31}$$

Due to the boundary conditions on the two vertical surfaces, n has to be an even integer, therefore, the eigenfunctions for each λ are

$$P_\lambda^{2j}(\mu) \sin(2j\tilde{\varphi}+h\pi/2) \quad \text{with} \quad 2j \leqq \lambda \tag{32}$$

where $\tilde{\varphi}=\varphi+3\pi/4$, $j=1, 2, \ldots$ for $h=0$ and $j=0, 1, 2, \ldots$ for $h=1$.

In the case of $h=0$, eq. (32) implies that $\lambda=1$ is not an eigenvalue because $2j>\lambda$ even for the smallest $j=1$. The smallest eigenvalue is therefore $\lambda=3$ and the corresponding eigenfunction is an even function, $P_3^2(\mu)\cos 2\varphi$. Corresponding to $\lambda=5$, there are two eigenfunctions: $P_5^2(\mu)\cos 2\varphi$ is even and $P_5^4 \sin 4\varphi$ is odd in φ. The multiplicity increases as λ increases subjected to the inequality $2j \leqq \lambda$ in eq. (32).

In the case of $h=1$, the smallest eigenvalue is $\lambda=0$ and the corresponding eigenfunction

TABLE 1

Eigenvalues between 0 *and* 3 *for a three-dimensional corner of a cube with boundary condition of the first kind,* $p=0$, $(h=0)$.

Even	Odd
0.453	
1.231	1.230
1.783	
2.117	2.117
2.515	2.514
3.0	

TABLE 2

Eigenvalues between 0 *and* 3 *for a three-dimensional corner of a cube with boundary condition of the second kind,* $\partial p/\partial n=0$, $(h=1)$.

Even	Odd
0.0	
0.840	0.840
1.206	
1.805	1.807
2.	2.
2.447	
2.814	2.814
2.959	2.869

$(j=0)$ is $P_0^0(\mu)=1$. Again the multiplicity increases as λ does. For example at $\lambda=4$, there are two even eigenfunctions $P_4^0(\mu)$ and $P_4^4(\mu)\cos 4\varphi$ with $j=0$, 2 and one odd eigenfunction $P_4^2(\mu)\sin 2\varphi$ with $j=1$.

The non-integer eigenvalues will be located by the aforementioned numerical procedure. For each eigenvalue so obtained, the first derivative of the characteristic determinant does not vanish, therefore, the corresponding coefficients A_m, C_j in the even eigenfunctions are defined by eqs. (25 and 27) and the coefficients B_m, D_j in the odd eigenfunctions are defined likewise.

All the eigenvalues between 0 and 3 are tabulated in tables 1 and 2 for the boundary condition of the first and of the second kind respectively. The coefficients A_m, C_j or B_m, D_j for the boundary condition of the second kind are tabulated in [7].

4. Conical Solution for the Incidence of a Plane Pulse

Fig. 4 shows a unit plane pulse incident on a corner of a cube, i.e., $\alpha=\pi/4$, $\beta=\pi/2$. The restriction of $\beta=\pi/2$ is essential so that the solution outside the unit sphere is two-dimensional. The restriction of $\alpha=\pi/4$ is not necessary. It is imposed to simplify the explanations of various regions and the explicit solutions [2] outside the unit sphere. The three edges are chosen as the three coordinate axes x_j with $j=2, 3, 4$ so that the solution due to the diffraction by j-th edge is appli-

cable to all three edges. The direction cosines of the normal to the incident pulse are designated as n_j with $n_2^2+n_3^2+n_4^2=1$. The equation for the plane of the incident pulse is

$$H_0 = n_2\bar{x}_2+n_3\bar{x}_3+n_4\bar{x}_4 = 1 \tag{33}$$

with $\bar{x}_j=x_j/(Ct)$. If the plane pulse hit the j-th edge first before hitting the vertex, n_j will be negative. This happens when the incident pulse diffracted by the first corner of the cube is subsequently diffracted by the adjacent corners. For the incidence on the first corner n_j's are non-negative, i.e.,

$$n_j \geqq 0, \qquad j=2, 3, 4\,. \tag{34}$$

In order to avoid the complicated discussion for various cases when one, two, or all of the n_j's are negative, the discussions in this section will be restricted to the case of eq. (34), i.e., for the incidence on the first corner of the cube.

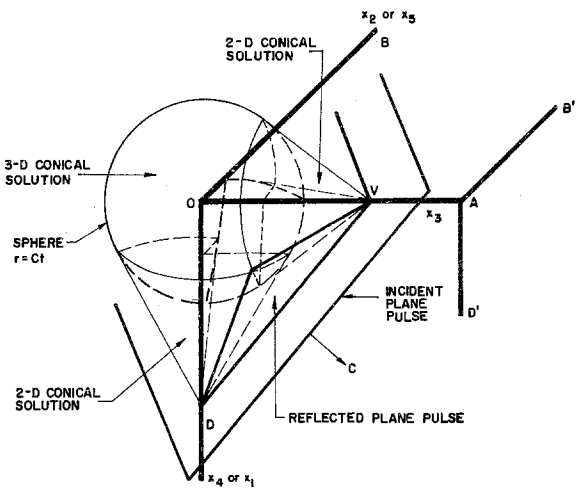

Figure 4. Oblique incidence of a plane pulse on a three-dimensional corner.

The plane pulse is intercepted by the j-axis at $X_j=1/n_j$, and intersects the $\bar{x}_j$–$\bar{x}_{j-1}$ plane along the line

$$n_{j-1}\bar{x}_{j-1}+n_j\bar{x}_j = 1 \tag{35}$$

For convenience, all the quantities with subscript 1 and 5 are introduced and identified with those with subscript 4 and 2 respectively.

The diffraction due to the j-th edge is confined inside the cone G_j with vertex at X_j on the $\bar{x}_j$ axis,

$$G_j\colon (1-n_j\bar{x}_j) > [(\bar{x}_{j-1})^2+(\bar{x}_{j+1})^2]^{\frac{1}{2}}(1-n_j^2)^{\frac{1}{2}}. \tag{36}$$

The diffraction by the vertex of the corner is confined inside the unit sphere

$$S\colon \bar{x}_2^2+\bar{x}_3^2+\bar{x}_4^2<1\,. \tag{37}$$

Outside the unit sphere the solutions are given by the two-dimensional conical solutions of Keller and Blank. The appropriated solutions are summarized in the next sub-section.

4.1. *Two-Dimensional Conical Solutions Outside the Unit Sphere*

The plane pulse will be reflected by the face, $\bar{x}_j=0$, (the $\bar{x}_{j-1}-\bar{x}_{j+1}$ plane) when $n_j>0$ and the plane of the reflected wave is

$$P_j = n_{j-1}\bar{x}_{j-1}-n_j\bar{x}_j+n_{j+1}\bar{x}_{j+1} = 1\,. \tag{38}$$

Across the reflected wave i.e., from $P_j>1$ to $P_j<1$, the solution jumps from unity to $1-(-1)^h$.

Inside the cone G_j but outside and ahead of the unit sphere S, the solution is given by the two-dimensional conical coordinates ξ_j and η_j with

$$\xi_j=\frac{\bar{x}_{j-1}(1-n_j^2)^{\frac{1}{2}}}{1-n_j\bar{x}_j} \quad \text{and} \quad \eta_j=\frac{-\bar{x}_{j+1}(1-n_j^2)^{\frac{1}{2}}}{1-n_j\bar{x}_j} \tag{39}$$

The cone G_j becomes the domain inside a unit circle, $\xi_j^2+\eta_j^2=1$. The reflected wave P_{j+1} in ξ, η variables becomes $\eta_{j-1}\xi_j+\eta_{j+1}\eta_j=(1-n_j^2)^{\frac{1}{2}}$ and is tangential to the unit circle at the point A_j^+ with polar coordinates $(1, \omega^+)$ where

$$\omega^+=\arcsin[n_{j+1}/(1-n_j^2)^{\frac{1}{2}}] \tag{40}$$

Similarly the reflected wave P_{j-1} is tangential to the unit circle at the point A_j^- with polar

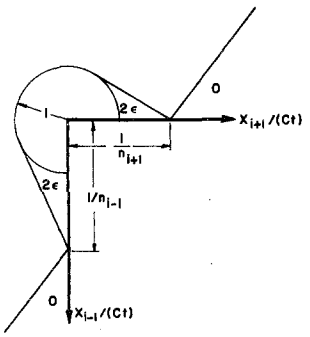

Figure 5. Section normal to the i-th axis for $h=1$.

coordinates $(1, \pi+\omega^+)$ as shown in Fig. 5. The boundary condition on the unit circle $\rho_j=1$, for p is

$$p=1-(-1)^h \quad \text{for} \quad \omega_j^+>\theta_j>0 \text{ and } 3\pi/2>\theta_j>\pi+\omega_j^+ \tag{41a}$$

and

$$p=1 \quad \text{for} \quad \omega_j^++\pi>\theta_j>\omega_j^+ . \tag{41b}$$

The disturbance pressure which lies inside the cone G_j but ahead of the unit sphere, i.e. $\bar{x}_{j+1}^2+\bar{x}_j^2+\bar{x}_{j-1}^2>1$ and $\bar{x}_j>n_j$, is given by the two-dimensional conical solution [2],

$$p=p_j(\rho_j, \theta_j)=\frac{1}{\pi}\arctan\frac{(1-\tilde{\rho}^2)\sqrt{3}}{4\tilde{\rho}\cos\frac{2}{3}\left(\theta_j+\omega_j^+ +\frac{\pi}{2}\right)-(1+\tilde{\rho}^2)}$$

$$-\frac{(-1)^h}{\pi}\arctan\frac{(1-\tilde{\rho}^2)\sqrt{3}}{4\tilde{\rho}\cos\frac{2}{3}\left(\theta_j-\omega_j^+ -\frac{\pi}{2}\right)-(1+\tilde{\rho}^2)} \tag{42}$$

where $\tilde{\rho}=\{\rho_j/[1+(1-\rho_j^2)^{\frac{1}{2}}]\}^{\frac{2}{3}}$ and the arctangent lies in the first and second quadrants.

In the domain common to adjacent cones, say cones G_j and G_{j+1}, but outside of the unit sphere S, the solution is

$$p=p_j(\rho_j, \theta_j)+p_{j+1}(\rho_{j+1}, \theta_{j+1})-h \tag{43}$$

In the domain ahead of the two cones G_j and G_{j+1} and behind the reflected wave P_{j-1}, the solution is

$$p=1-(-1)^h \tag{44}$$

In the remaining domains outside the unit sphere, i.e., when eqs. (42, 43, and 44) are not applicable, the solution is that of the incident pulse alone, which is

$$p=0 \quad \text{for} \quad H_0>1$$
$$p=1 \quad \text{for} \quad H_0<0\,. \tag{45}$$

Equations (42) to (45) define the solution outside the unit sphere and the boundary data $F(\mu, \varphi)$ on the unit sphere due to the continuity of the solution.

4.2. *The Three-Dimensional Conical Solution*

As outlined in section 2, the conical solution inside the unit sphere is represented by the eigenfunction expansions,

$$p(\zeta, \mu, \varphi)=\sum_{\lambda} K_\lambda Z_\lambda(\zeta)\, G_\lambda(\mu, \varphi) \tag{46}$$

where

$$\zeta = r/(Ct)=(\bar{x}_2^2+\bar{x}_3^2+\bar{x}_4^2)^{\frac{1}{2}},\ \bar{x}_4=-\zeta\mu$$
$$\bar{x}_2=\zeta(1-\mu^2)^{\frac{1}{2}}\sin(\varphi-3\pi/2) \text{ and } \bar{x}_3=\zeta(1-\mu^2)^{\frac{1}{2}}\cos(\varphi-3\pi/2)\,.$$

The eigenvalues λ's and the eigenfunction G_λ are determined in section 3. The function $Z_\lambda(\zeta)$ is a solution of the differential equation (6), i.e.,

$$\zeta^2(1-\zeta^2)Z''(\zeta)+2(1-\zeta^2)\zeta Z'(\zeta)-\lambda(\lambda+1)Z(\zeta)=0\,. \tag{47}$$

The boundary conditions are $Z(0)<\infty$ and $Z(1)=1$. The latter condition on the unit sphere $\zeta=1$ permits the determination of the coefficients K_λ from the boundary data $F(\mu, \varphi)$ on the unit sphere without the knowledge of $Z_k(\zeta)$. The equation for the coefficient K_λ is

$$K_\lambda=\tfrac{1}{2}\int_0^{\mu_0} d\mu \int_{-\pi}^{\pi} d\varphi\, F(\mu, \varphi)\, G_\lambda^+(\mu, \varphi)+\tfrac{1}{2}\int_{\mu_0}^{\pi} d\mu \int_{\pi+\alpha}^{\pi-\alpha} d\varphi\, F(\mu, \varphi)\, G_\lambda^-(\mu, \varphi) \tag{48}$$

The factor $\frac{1}{2}$ is due to the normalization condition of eq. (12b) for G_λ in which the integration with respect to φ is carried over only half the interval. In the numerical determination of K_λ the double integral can be reduced to a sum of line integrals. For example, eq. (35) for an even eigenfunction becomes

$$K_\lambda=\sum_{m=0,1}^{M_e}\int_{\mu_0}^{1} A_m P_\lambda^{-m}(\mu) f_m^+(\mu)\,d\mu+\sum_{j=0,1}^{J_e}\int_{-1}^{\mu_0} C_j P_\lambda^{-\nu_j}(-\mu) f_j^-(\mu)\,d\mu \tag{49}$$

where

$$f_m^+(\mu)=\tfrac{1}{2}\int_{-\pi}^{\pi} F(\mu, \varphi)\cos m\varphi\, d\varphi, f_j^-(\mu)=\tfrac{1}{2}\int_{-\Phi/2}^{\Phi/2} F(\mu, \varphi)\cos \nu_j\varphi\, d\varphi\,,$$

and

$$\nu_j=(2j+1-h)\pi/\Phi\,.$$

Similarly, the coefficient K_λ for an odd eigenfunction can also be written as a sum of line integrals.

For the determination of the conical solution inside the unit sphere, it is necessary to construct the solution $Z_\lambda(\zeta)$ of the differential eq. (47), subjected to the boundary conditions at $\zeta=0$ and $\zeta=1$. The solution is obtained numerically by the "shooting method". For Z_λ to be finite at $\xi=0$, the solution can be represented by the power series,

$$Z(\zeta)=a_0\zeta^\lambda\left[1+\frac{\lambda(\lambda+1)}{4\lambda+6}\zeta^2+\ \ldots\right] \tag{50}$$

By setting $a_0=1$, the differential equation can be integrated numerically from a small ζ_0 (say 0.001) with initial data $\tilde{Z}_\lambda(\zeta_0)=\zeta_0^\lambda[1+\lambda(\lambda+1)\zeta_0^2/(4\lambda+6)]$ and $\tilde{Z}'_\lambda(\zeta_0)=\lambda\zeta_0^{\lambda-1}[1+(\lambda+1)(\lambda+2)\zeta_0^2/(4\lambda+6)]$. The numerical integration for $\tilde{Z}_\lambda(\zeta)$ is continued until ζ is close to 1 (say

0.99). For the determination of $\tilde{Z}_\lambda(1)$, the values of $\tilde{Z}_\lambda(\zeta)$ and $\tilde{Z}'_\lambda(\zeta)$ at the last station are matched with those given by the series solution of $1-\zeta$, i.e.,

$$\tilde{Z}_\lambda(\zeta) = \tilde{Z}_\lambda(1)\left\{1 + \frac{\lambda(\lambda+1)}{3}(1-\zeta)\log(1-\zeta)[1+O(1-\zeta)]\right\} + a_1(1-\zeta)\{1+O(1-\zeta)\} \tag{51}$$

Since the problem is linear, the correct solution is $Z_\lambda(\zeta) = \tilde{Z}_\lambda(\zeta)/\tilde{Z}_\lambda(1)$ and the correct value for a_0 in eq. (50), which is needed to start the numerical integration, is $1/\tilde{Z}_\lambda(1)$. Thus for a given boundary data $F(\mu, \varphi)$ on the unit sphere, the conical solution inside the unit sphere is defined.

4.3. *Numerical Examples*

A numerical program is listed in [8] for $h=1$. For a given incident direction (n_2, n_3, n_4), the program computes (i) the solution in the appropriate regions outside the unit sphere as described in sect. 4.1, (ii) the boundary data $F(\mu, \varphi)$ on the unit sphere and the coefficients K_λ in eq. (46) and (iii) the solution $p(\zeta, \mu, \varphi)$ inside the unit sphere as described in sect. 4.2.

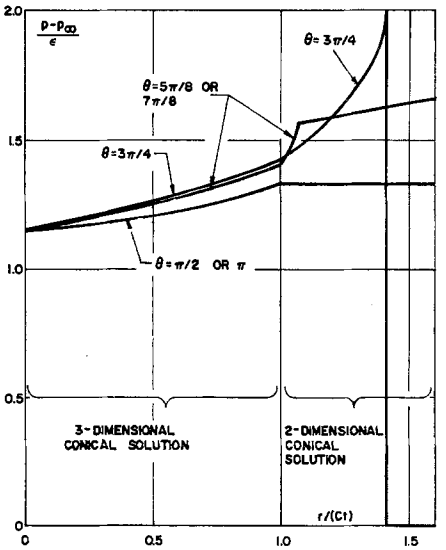

Figure 6. Over pressure along constant θ lines on face OAD ($\varphi = 3\pi/4$) with plane pulse advancing along OB (1, 0, 0).

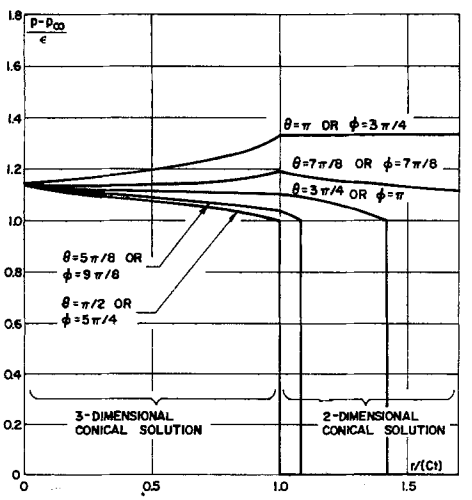

Figure 7. Over pressure along constant φ lines on face OAB ($\theta = \pi/2$) and along constant θ lines on face OBD ($\varphi = -3\pi/4$).

Figures 6 and 7 show the pressure distribution on the three faces of a rigid corner of a cube due to the normal incidence of a plane acoustic pulse ($n_2=1, n_3=0, n_4=0$). The boundary condition is of the second kind ($h=1$). The discontinuities in the slope of the pressure distribution indicate the crossing of a characteristic sphere or cone. The results confirm with less than 1% variation the symmetry of the solution with respect to the plane bisecting the two faces OAB and OAD which are normal to the incident plane pulse. The value at the vertex is within 0.1% of the value 8/7 which is predicted by the "mean-value" theorem [7, 9] to be the ratio of 4π to the solid angle outside the corner i.e. $4\pi(1-\frac{1}{8})$. For the solution inside the unit sphere the calculations are performed with eigenvalues less than or equal to 3. When the calculations are performed with only eigenvalues less than or equal to 2 the result differs from those in the figures within 6%.

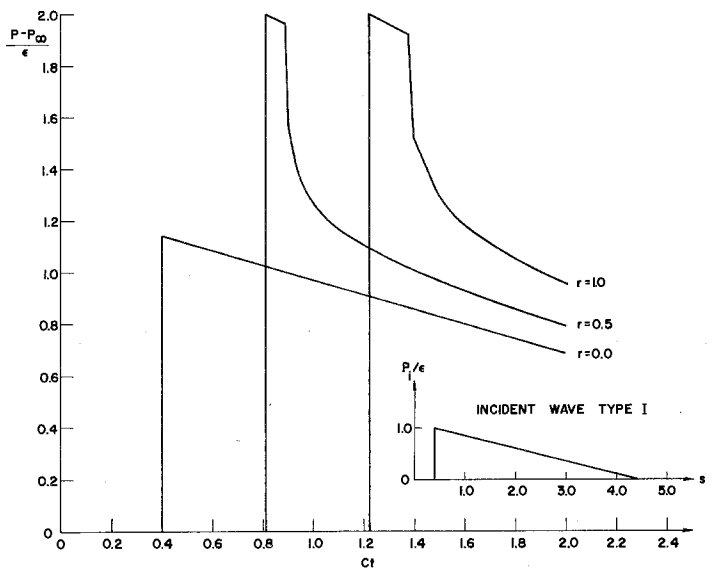

Figure 8. Pressure signature received at points along the line $\theta=\pi/2, \varphi=\pi$ for plane wave incident at equal angles with the edges and with wave form of type I.

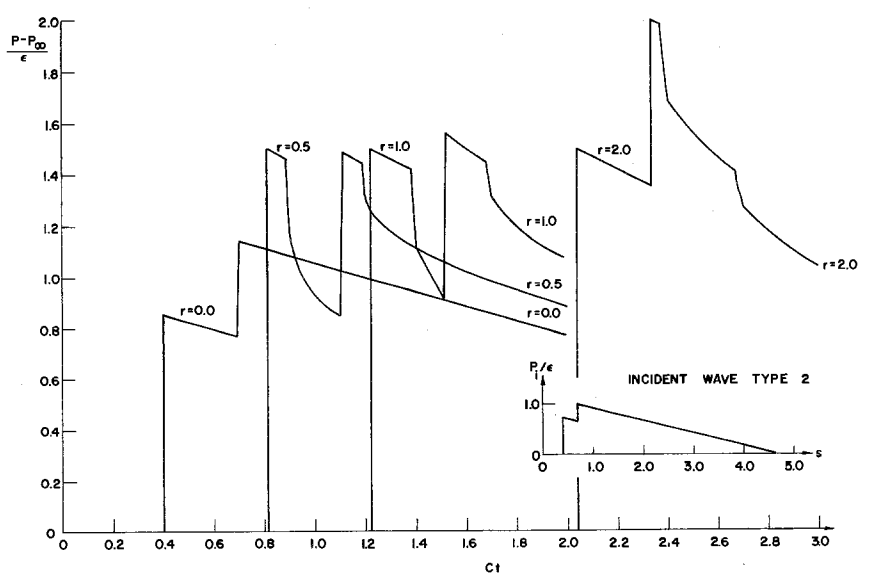

Figure 9. Pressure signature received at points along the line $\theta=\pi/2, \varphi=\pi$ for plane wave incident at equal angles with the edges and with wave form of type 2.

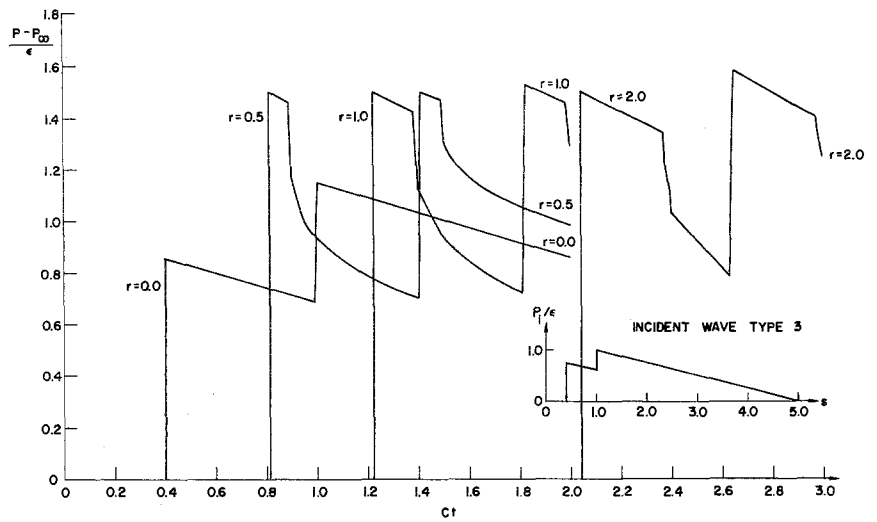

Figure 10. Pressure signature received at points along line $\theta=\pi/2$, $\varphi=\pi$ for plane wave incident at equal angles with the edges and with wave form of type 3.

5. Incidence of a Plane Wave

An incident plane wave p_i can be represented in general as $p_i=\psi(s)$ with $s=Ct-(n_2x_2+n_3x_3+n_4x_4)$ where the wave form ψ is a given function of its phase s and n_j's are the direction cosines.

When the wave form is a Heaviside function, the diffraction due to the three-dimensional corner is given by the conical solution described in the preceding section. It will be designated as $p^*(r/(Ct), \mu, \varphi)$. The solution corresponding to a plane wave of wave form $\psi(\eta)$ is given by the Stieltjes integral

$$p(r, \theta, \varphi, t) = \int p^*\left(\frac{r}{Ct-\eta}, \mu, \varphi\right) d\psi(\eta) = \sum_j p^*\left[\frac{r}{Ct-\eta_j}\right]\left[\psi(\eta_{j+1})-\psi(\eta_j)\right] \tag{52}$$

The second form is employed in the numerical program in [8] for the computation of the solution at points on the surface of the corner.

In the evaluation of pressure load on structures due to the incidence of a sonic boom, the incident wave can be locally represented as a plane wave since the length of a structure is usually much smaller than the radius of curvature of the wave front. The wave form ψ is in general a sequence of a weak shock wave and an expansive wave or a compression wave as shown in the inserts in Figs. 8, 9 and 10. Numerical results shown in those figures are carried out for the waves incident at equal angles to the edges, i.e. $n_2=n_3=n_4=1/\sqrt{3}$. The curves show the pressure signature at points $r=0$, 0.5, 1, 2 along the line dividing the top surface of the corner ($\mu=0$, $\varphi=\pi$).

The incident wave in Fig. 8 is a simple N-wave in sonic boom problems with front shock strength ε. The length of the N-wave, which is 4, is nearly the length of an airplane. The unit length scale in the numerical examples is therefore of the order of hundreds of feet. As shown in the figure, the pressure signature at the vertex is $\frac{8}{7}$ times the incident wave form in agreement with the theorem stated in [7.9]. At the point $r=0.5$, the front part of the pressure signature is equal to 2ε i.e., the same as a regular reflection and then decreases from the value of a regular reflection after the arrival of the diffracted waves from the edges and corner. Similar phenomenon is observed for the pressure signature at $r=1$ with a relative delay in the arrival of the diffracted waves.

In Fig. 9, the front shock is split into two shock waves jointed by the expansion wave of thickness 0.3. Although the peak incident pressure is the same as that in the single shock, the peak pressure received at points $r=0.5$ and 1.0 are nearly 25% less than that in the case of

regular reflection. The peak pressure at the point $r=2.0$ does reach the value of regular reflection, i.e. 2ε.

In Fig. 10, the front shock is split into two shocks separated by an expansion wave of thickness 0.6. The peak pressure for all three points are now nearly 25% less than the value 2ε in a regular reflection.

Figs. 9 and 10 demonstrate that when the diffracted wave front arrives prior to the arrival of the peak incident wave, the local peak pressure can be much less than the value given by a regular reflection. Since the length scale in the incident wave form is one quarter of the length of an airplane. The area on the surface of the corner where there is such a reduction in peak pressure is significant (of the order of hundreds of square feet). Additional examples are presented in [8].

6. Concluding Remarks

In this paper the conical solution for the diffraction of a plane pulse by a three-dimensional corner is presented for boundary conditions of the first kind $p=0$ and also for that of the second kind $p_n=0$. By the decomposition of a plane wave to plane pulses, the solution for the diffraction of a plane wave is obtained by superposition of the conical solutions.

In the construction of the conical solution by separation of variables, an eigenvalue problem in spherical angle variables is formulated and solved in sections 2 and 3. The technique for the solution of the eigenvalue problem is applicable to a more general shape of boundary on the unit sphere formed by two great circles of given longitudes and a horizontal circle of given latidude.

The solutions of the eigenvalue problem in spherical angles for the conical problem remain the same and therefore can be used for potential or unsteady heat conduction problems, so long as the boundary conditions in the θ–φ plane are the same.

The solutions of the eigenvalue problem remain the same for a generalized conical solution in the construction of a general diffraction solution. When the boundary data on the unit sphere around the vertex of a three-dimensional corner is now a function of t in addition to the spherical angles θ and φ, it can be written as a power series with respect to t, i.e., $F(t, \theta, \varphi) = \Sigma_\gamma t^\gamma F_\gamma(\theta, \varphi)$ for $t>0$ where the summation is carried over a sequence of positive numbers, $\gamma \geqq 0$. The solution inside the unit sphere can likewise be written as $p(t, r, \theta, \varphi) = \Sigma_\gamma t^\gamma p^{(\gamma)}(\zeta, \theta, \varphi)$. For each γ the wave equation yields the governing equation for $p^{(\gamma)}(\zeta, \theta, \varphi)$, the generalized conical solution, subjected to the boundary condition on the unit sphere $p^{(\gamma)}(\zeta, \theta, \varphi) = F_\gamma(\theta, \varphi)$, while the boundary conditions on the surfaces of the corner remain the same as eqs. (3,4).

Since the differential operators with respect to θ and φ are independent of γ, the corresponding eigenvalue problem in θ–φ plane after the separation of the variable ζ is the same as that for $\gamma=0$, i.e., the conical problem. The solution $p^{(\gamma)}$ can therefore be written as, $p^{(\gamma)}(\zeta, \theta, \varphi) = \Sigma_\lambda K_\lambda^{(\gamma)} Z_\lambda^{(\gamma)}(\zeta) G_\lambda(\mu, \varphi)$. The eigenvalues λ's and the eigenfunctions $G_\lambda(\mu, \varphi)$ are identical with those obtained for $\gamma=0$ in section 3. With the boundary condition $Z_\lambda^{(\gamma)}(1) = 1$ imposed on $Z_\lambda^{(\gamma)}$, the constants $K_\lambda^{(\gamma)}$ are also related to the boundary data $F_\gamma(\mu, \theta)$ by the same equation, eq. (48), and can be determined by the same numerical program independent of γ. The appearance of γ occurs only in the differential equation for $Z_\lambda^{(\gamma)}(\zeta)$ which is

$$\zeta^2(1-\zeta^2)\frac{d^2Z}{d\zeta^2} + 2\zeta[1+(\gamma-1)\zeta^2]\frac{dZ}{d\zeta} - [\gamma(\gamma-1)\zeta^2+\lambda(\lambda+1)]Z = 0\,.$$

The boundary conditions are the same for all γ, i.e., $Z(1)=1$ and $Z(0)$ is finite. $Z_\lambda^{(\gamma)}(\zeta)$ can be determined by the same procedure described in sect. 4.3 for $\gamma=0$.

References 7 and 8 present more detail description of the analysis for the boundary condition of the second kind only. They contain more numerical examples and all the relevant numerical programs.

Acknowledgment

The authors wish to acknowledge Professor Antonio Ferri, Director of the Aerospace Laboratory, and Professor J. B. Keller, Head of the Department of Mathematics, New York University, Bronx, New York for their valuable discussions.

REFERENCES

[1] F. G. Friedlander, *Sound Pulse*, Cambridge University Press, (New York), New York (1958).
[2] J. B. Keller and A. Blank, Diffraction and Reflection of Pulses by Wedges and Corners, *Communication on Pure and Applied Mechanics*, 4, 1, (1951) 75–94.
[3] R. K. Luneberg, *Mathematical Theory of Optics*, Brown University Lecture Notes (1944).
[4] A. Busemann, Infinitesimale kegelige Überschall-strömung, *Schriften der Deutschen Akademie für, Luftfahrtforschung*, 7B, 3, (1943) (Transl. NACA TM 1100) 105–122.
[5] E. W. Hobson, *The Theory of Spherical and Ellipsoidal Harmonics*, Chelsea Publishing Company, (New York), New York, (1955) 178–190.
[6] R. V. Churchill, *Complex Variables and Applications*, 2nd Ed. McGraw Hill Company, (New York), New York, (1960) 218–229.
[7] L. Ting and F. Kung, *Diffraction of a Pulse by a Three-Dimensional Corner*, NASA Contractor Report CR-1728, (Washington), D.C. (1971)
[8] L. Ting and F. Kung, *Diffraction of a Plane Wave by a Three-Dimensional Corner*, Rept. NYU-AA-70-28, New York University, (1971).
[9] L. Ting, On the Diffraction of an Arbitrary Pulse by a Wedge or a Cone, *Quarterly of Applied Mathematics*, XVIII, 1, (1960) 89–92.